Progress In Electromagnetics Research, Vol. 127, 389–404, 2012

THE REFLECTION AND TRANSMISSION OF ELECTROMAGNETIC WAVES BY A UNIAXIAL CHIRAL SLAB

J.-F. Dong* **and J. Li**

Institute of Optical Fiber Communication and Network Technology, Ningbo University, Ningbo 315211, China

Abstract—The reflection and transmission of electromagnetic waves obliquely incident on a uniaxial chiral slab with the optical axis perpendicular to the interface have been investigated. Firstly, the formulas of the reflection and transmission are derived. Then numerical results for four cases of the uniaxial chiral media are presented and different chiral parameters are considered. Finally, the Brewster's angles and total transmission are discussed.

1. INTRODUCTION

The chiral metamaterials have attracted a lot of attention in the last decade. The theoretical [1–3] and experimental (or simulative) [4–11] studies have demonstrated that the negative refractive indices can be realized in the chiral metamaterials. It is also shown theoretically that a chiral slab with negative refractive index can be used as a perfect lens which provides subwavelength resolution for circularly polarized waves [12, 13]. Many related studies on the chiral metamaterials have been published [14–22], and several applications such as waveguides [23–28], polarization rotator [29, 30], cloaking [31], and antennas [32] using chiral metamaterials have been proposed and investigated. However, these studies focus on the isotropic chiral medium. Usually, uniaxially anisotropic chiral medium is quite easy to be realized artificially [33–35]. Recently, Cheng and Cui [35] investigated negative refractions in uniaxially anisotropic chiral media. They found that the condition to realize the negative refraction in uniaxial chiral media could be quite loose. They also investigated the

Received 17 March 2012, Accepted 20 April 2012, Scheduled 27 April 2012

* Corresponding author: Jianfeng Dong (dongjianfeng@nbu.edu.cn).

reflection and refraction properties of plane waves incident from free space into a uniaxially anisotropic chiral medium, and the Brewster's angles have been obtained numerically [36]. Guided modes in uniaxial chiral circular waveguides have been studied [37]. The uniaxial chiral media may find potential applications for the design of microwave and optical devices such as polarizers and beam splitters.

On the other hand, the reflection and transmission of electromagnetic waves obliquely and normally incident on the isotropic chiral media and chiral slab have been examined in literature [38–42]. The effective chirality parameter of the C_4-symmetry chiral metamaterial has been retrieved employing the transmission and reflection coefficients at normal incidence [43]. The reflection and transmission by the uniaxial chiral slab with optical axis parallel to the interfaces for normal incident waves have also been investigated [44, 45]. One application of the uniaxial chiral slab is a polarization transformer [46]. However, the reflection and transmission by the uniaxial chiral slab for obliquely incident waves have not been considered yet, and the possibility of negative electromagnetic parameter has not been discussed. In this paper, we investigate the reflection and transmission of electromagnetic waves by a uniaxially chiral medium slab with the optical axis perpendicular to the interface. The formulas of the reflection and transmission are obtained, numerical examples for four cases of electromagnetic parameters of uniaxial chiral media are given, and different chiral parameters are considered.

2. FORMULATIONS

The constitutive relations in the uniaxial chiral medium are (time-harmonic field with $e^{j\omega t}$ is assumed and suppressed) [33]:

$$\mathbf{D} = \left[\varepsilon_t \bar{\bar{I}}_t + \varepsilon_z \hat{\mathbf{z}}\hat{\mathbf{z}}\right] \cdot \mathbf{E} - j\kappa\sqrt{\mu_0\varepsilon_0}\, \hat{\mathbf{z}}\hat{\mathbf{z}} \cdot \mathbf{H} \tag{1}$$

$$\mathbf{B} = \left[\mu_t \bar{\bar{I}}_t + \mu_z \hat{\mathbf{z}}\hat{\mathbf{z}}\right] \cdot \mathbf{H} + j\kappa\sqrt{\mu_0\varepsilon_0}\, \hat{\mathbf{z}}\hat{\mathbf{z}} \cdot \mathbf{E} \tag{2}$$

where $\hat{\mathbf{z}}$ is a unit vector along z direction which is the optical axial direction of the uniaxial chiral medium, and $\bar{\bar{I}}_t = \hat{\mathbf{x}}\hat{\mathbf{x}} + \hat{\mathbf{y}}\hat{\mathbf{y}}$. $\varepsilon_t(\mu_t)$ and $\varepsilon_z(\mu_z)$ are the permittivity (permeability) of the uniaxial chiral medium perpendicular to the optical axial (transversal) and the optical axial (longitudinal) direction, respectively; ε_0 and μ_0 are the permittivity and permeability of free space. κ is the chirality parameter, which describes electromagnetic coupling.

There are two eigenwaves in the uniaxial chiral medium whose wavenumbers are [33]: $k_\pm = \frac{\omega\sqrt{\varepsilon_t\mu_t}}{\sqrt{\cos^2\theta_\pm + \sin^2\theta_\pm/A_\pm}}$, with $A_\pm =$

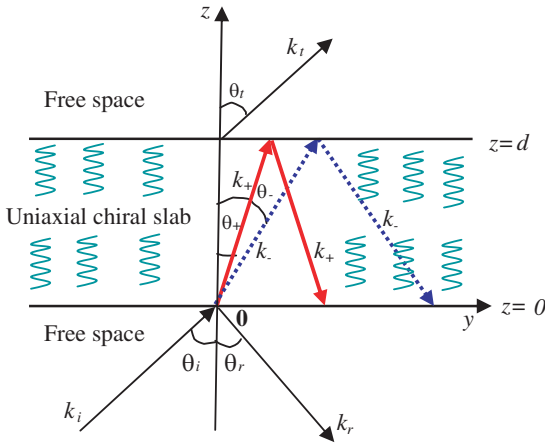

Figure 1. Oblique incidence of a plane electromagnetic wave on an infinite uniaxial chiral slab with the optical axis perpendicular to the interface.

$\frac{1}{2}\left(\frac{\mu_z}{\mu_t}+\frac{\varepsilon_z}{\varepsilon_t}\right)\pm\sqrt{\frac{1}{4}\left(\frac{\mu_z}{\mu_t}-\frac{\varepsilon_z}{\varepsilon_t}\right)^2+\frac{\kappa^2\mu_0\varepsilon_0}{\mu_t\varepsilon_t}}$, $\theta_\pm$ are the angles between the optical axial direction and propagation direction of the eigenwaves.

Consider an infinite uniaxial chiral slab of thickness d, with the optical axial perpendicular to the interface as shown in Fig. 1. A plane electromagnetic wave obliquely incidents upon the uniaxial chiral slab. The incident angle is θ_i, the reflected and transmitted angles are θ_r and θ_t, the refraction angles in the uniaxial chiral slab are θ_+, θ_- for two eigenwaves. The wavenumbers of the incident, reflected and transmitted waves are k_i, k_r, and k_t. $k_t = k_r = k_i = k_0 = \omega\sqrt{\mu_0\varepsilon_0}$, $\theta_t = \theta_r = \theta_i$.

In the region $z \leq 0$, the incident plane electromagnetic wave can be expressed as:

$$\mathbf{E}_i = \mathbf{E}_{0i}e^{-jk_i(y\sin\theta_i+z\cos\theta_i)}, \qquad \mathbf{H}_i = \mathbf{H}_{0i}e^{-jk_i(y\sin\theta_i+z\cos\theta_i)} \tag{3}$$

where

$$\begin{aligned}\mathbf{E}_{0i} &= E_{i\perp}\hat{\mathbf{x}} + E_{i\parallel}\left(\hat{\mathbf{y}}\cos\theta_i - \hat{\mathbf{z}}\sin\theta_i\right),\\ \mathbf{H}_{0i} &= \eta_0^{-1}\left[-E_{i\parallel}\hat{\mathbf{x}} + E_{i\perp}\left(\hat{\mathbf{y}}\cos\theta_i - \hat{\mathbf{z}}\sin\theta_i\right)\right].\end{aligned} \tag{4}$$

$\eta_0=\sqrt{\mu_0/\varepsilon_0}$, subscripts $\perp$, $\parallel$ represent perpendicular (TE) and parallel (TM) components of the plane electromagnetic wave, respectively.

The reflected electromagnetic fields can be written as:

$$\mathbf{E}_r = \mathbf{E}_{0r}e^{-jk_r(y\sin\theta_r-z\cos\theta_r)}, \qquad \mathbf{H}_r = \mathbf{H}_{0r}e^{-jk_r(y\sin\theta_r-z\cos\theta_r)}. \tag{5}$$

where

$$\begin{aligned}\mathbf{E}_{0r} &= E_{r\perp}\hat{\mathbf{x}} - E_{r\parallel}\left(\hat{\mathbf{y}}\cos\theta_r + \hat{\mathbf{z}}\sin\theta_r\right),\\ \mathbf{H}_{0r} &= \eta_0^{-1}\left[-E_{r\parallel}\hat{\mathbf{x}} - E_{r\perp}\left(\hat{\mathbf{y}}\cos\theta_r + \hat{\mathbf{z}}\sin\theta_r\right)\right].\end{aligned} \tag{6}$$

There are four electromagnetic waves in the uniaxial chiral slab ($0 \le z \le d$), two propagating towards the interface $z = d$ and the other two propagating towards the interface $z = 0$, as shown in Fig. 1. The electromagnetic fields of the two waves propagating towards the interface $z = d$ can be represented as:

$$\begin{aligned}\mathbf{E}_c^+ &= \mathbf{E}_{01}^+ e^{-jk_+(y\sin\theta_+ + z\cos\theta_+)} + \mathbf{E}_{02}^+ e^{-jk_-(y\sin\theta_- + z\cos\theta_-)},\\ \mathbf{H}_c^+ &= \mathbf{H}_{01}^+ e^{-jk_+(y\sin\theta_+ + z\cos\theta_+)} + \mathbf{H}_{02}^+ e^{-jk_-(y\sin\theta_- + z\cos\theta_-)}.\end{aligned} \tag{7}$$

where

$$\begin{aligned}\mathbf{E}_{01}^+ &= E_{01}^+\left(\omega\mu_t Y_{z+}\hat{\mathbf{x}} + k_z^+\hat{\mathbf{y}} - \frac{k_y^+}{A_+}\hat{\mathbf{z}}\right),\\ \mathbf{E}_{02}^+ &= E_{02}^+\left(\omega\mu_t Y_{z-}\hat{\mathbf{x}} + k_z^-\hat{\mathbf{y}} - \frac{k_y^-}{A_-}\hat{\mathbf{z}}\right),\\ \mathbf{H}_{01}^+ &= E_{01}^+ Y_{z+}\left[-\omega\varepsilon_t Z_{z+}\hat{\mathbf{x}} + k_z^+\hat{\mathbf{y}} - \frac{k_y^+}{A_+}\hat{\mathbf{z}}\right],\\ \mathbf{H}_{02}^+ &= E_{02}^+ Y_{z-}\left[-\omega\varepsilon_t Z_{z-}\hat{\mathbf{x}} + k_z^-\hat{\mathbf{y}} - \frac{k_y^-}{A_-}\hat{\mathbf{z}}\right].\end{aligned} \tag{8}$$

with $k_y^\pm = k_\pm\sin\theta_\pm$, $k_z^\pm = k_\pm\cos\theta_\pm$, $Y_{z\pm} = \frac{\varepsilon_t}{-j\kappa\sqrt{\mu_0\varepsilon_0}}\left(A_\pm - \frac{\varepsilon_z}{\varepsilon_t}\right)$, $Z_{z\pm} = \frac{1}{Y_{z\pm}} = \frac{\mu_t}{j\kappa\sqrt{\mu_0\varepsilon_0}}\left(A_\pm - \frac{\mu_z}{\mu_t}\right)$ [33].

The electromagnetic fields of the two waves propagating towards the interface $z = 0$ can be represented as:

$$\begin{aligned}\mathbf{E}_c^- &= \mathbf{E}_{01}^- e^{-jk_+[y\sin\theta_+ - (z-d)\cos\theta_+]} + \mathbf{E}_{02}^- e^{-jk_-[y\sin\theta_- - (z-d)\cos\theta_-]},\\ \mathbf{H}_c^- &= \mathbf{H}_{01}^- e^{-jk_+[y\sin\theta_+ - (z-d)\cos\theta_+]} + \mathbf{H}_{02}^- e^{-jk_-[y\sin\theta_- - (z-d)\cos\theta_-]}.\end{aligned} \tag{9}$$

where

$$\begin{aligned}\mathbf{E}_{01}^- &= E_{01}^-\left(\omega\mu_t Y_{z+}\hat{\mathbf{x}} - k_z^+\hat{\mathbf{y}} - \frac{k_y^+}{A_+}\hat{\mathbf{z}}\right),\\ \mathbf{E}_{02}^- &= E_{02}^-\left(\omega\mu_t Y_{z-}\hat{\mathbf{x}} - k_z^-\hat{\mathbf{y}} - \frac{k_y^-}{A_-}\hat{\mathbf{z}}\right).\end{aligned}$$

$$\mathbf{H}_{01}^{-} = E_{01}^{-}Y_{z+}\left[-\omega\varepsilon_t Z_{z+}\hat{\mathbf{x}} - k_z^{+}\hat{\mathbf{y}} - \frac{k_y^{+}}{A_{+}}\hat{\mathbf{z}},\right],$$

$$\mathbf{H}_{02}^{-} = E_{02}^{-}Y_{z-}\left[-\omega\varepsilon_t Z_{z-}\hat{\mathbf{x}} - k_z^{-}\hat{\mathbf{y}} - \frac{k_y^{-}}{A_{-}}\hat{\mathbf{z}}\right]. \tag{10}$$

In the region $z \geq d$, the transmitted electromagnetic fields can be written as:

$$\mathbf{E}_t = \mathbf{E}_{0t}e^{-jk_t[y\sin\theta_t+(z-d)\cos\theta_t]}, \quad \mathbf{H}_t = \mathbf{H}_{0t}e^{-jk_t[y\sin\theta_t+(z-d)\cos\theta_t]} \tag{11}$$

where

$$\mathbf{E}_{0t} = E_{t\perp}\hat{\mathbf{x}} + E_{t\parallel}\left(\hat{\mathbf{y}}\cos\theta_t - \hat{\mathbf{z}}\sin\theta_t\right),$$

$$\mathbf{H}_{0t} = \eta_0^{-1}\left[-E_{t\parallel}\hat{\mathbf{x}} + E_{t\perp}\left(\hat{\mathbf{y}}\cos\theta_t - \hat{\mathbf{z}}\sin\theta_t\right)\right]. \tag{12}$$

According to the boundary conditions of the electromagnetic fields at interfaces $z = 0$ and $z = d$:

$$\begin{cases} [\mathbf{E}_i(0) + \mathbf{E}_r(0)]_t = [\mathbf{E}_c^{+}(0) + \mathbf{E}_c^{-}(0)]_t \\ [\mathbf{H}_i(0) + \mathbf{H}_r(0)]_t = [\mathbf{H}_c^{+}(0) + \mathbf{H}_c^{-}(0)]_t \\ [\mathbf{E}_t(d)]_t = [\mathbf{E}_{\mathbf{c}}^{+}(d) + \mathbf{E}_{\mathbf{c}}^{-}(d)]_t \\ [\mathbf{H}_t(d)]_t = [\mathbf{H}_c^{+}(d) + \mathbf{H}_c^{-}(d)]_t \end{cases} \tag{13}$$

where $[\ \ ]_t$ represents tangent components of the electromagnetic fields.

Obviously, $k_{\pm}\sin\theta_{\pm} = k_0\sin\theta_i$. Using $k_{\pm} = \frac{\omega\sqrt{\varepsilon_t\mu_t}}{\sqrt{\cos^2\theta_{\pm}+\sin^2\theta_{\pm}/A_{\pm}}}$, we can find the refraction angles $\theta_{\pm}$ [36]. Then $k_z^{\pm} = k_{\pm}\cos\theta_{\pm}$ can be obtained. The eight unknowns, $E_{r\perp}$, $E_{r\parallel}$, E_{01}^{+}, E_{02}^{+}, E_{01}^{-}, E_{02}^{-}, $E_{t\perp}$ and $E_{t\parallel}$ can be related with incident electromagnetic fields amplitudes $E_{i\perp}$, $E_{i\parallel}$ as following:

$$\begin{bmatrix} E_{r\perp} \\ E_{r\parallel} \\ E_{01}^{+} \\ E_{02}^{+} \\ E_{01}^{-} \\ E_{02}^{-} \\ E_{t\perp} \\ E_{t\parallel} \end{bmatrix} = Q^{-1}\begin{bmatrix} E_{i\perp} \\ E_{i\parallel} \\ E_{i\parallel} \\ E_{i\perp} \\ 0 \\ 0 \\ 0 \\ 0 \end{bmatrix} \tag{14}$$

where Q is the matrix:

$$
Q = \begin{pmatrix}
-1 & 0 & \omega\mu_t Y_{z+} & \omega\mu_t Y_{z-} \\
0 & 1 & \frac{k_z^+}{\cos\theta_i} & \frac{k_z^-}{\cos\theta_i} \\
0 & -1 & \eta_0\omega\varepsilon_t & \eta_0\omega\varepsilon_t \\
1 & 0 & \frac{\eta_0 k_z^+ Y_{z+}}{\cos\theta_i} & \frac{\eta_0 k_z^- Y_{z-}}{\cos\theta_i} \\
0 & 0 & \omega\mu_t Y_{z+} e^{-jk_z^+ d} & \omega\mu_t Y_{z-} e^{-jk_z^- d} \\
0 & 0 & \frac{k_z^+}{\cos\theta_i} e^{-jk_z^+ d} & \frac{k_z^-}{\cos\theta_i} e^{-jk_z^- d} \\
0 & 0 & \eta_0\omega\varepsilon_t e^{-jk_z^+ d} & \eta_0\omega\varepsilon_t e^{-jk_z^- d} \\
0 & 0 & \frac{\eta_0 k_z^+ Y_{z+}}{\cos\theta_i} e^{-jk_z^+ d} & \frac{\eta_0 k_z^- Y_{z-}}{\cos\theta_i} e^{-jk_z^- d}
\end{pmatrix}
$$

$$
\begin{pmatrix}
\omega\mu_t Y_{z+} e^{-jk_z^+ d} & \omega\mu_t Y_{z-} e^{-jk_z^- d} & 0 & 0 \\
-\frac{k_z^+}{\cos\theta_i} e^{-jk_z^+ d} & -\frac{k_z^-}{\cos\theta_i} e^{-jk_z^- d} & 0 & 0 \\
\eta_0\omega\varepsilon_t e^{-jk_z^+ d} & \eta_0\omega\varepsilon_t e^{-jk_z^- d} & 0 & 0 \\
-\frac{\eta_0 k_z^+ Y_{z+}}{\cos\theta_i} e^{-jk_z^+ d} & -\frac{\eta_0 k_z^- Y_{z-}}{\cos\theta_i} e^{-jk_z^- d} & 0 & 0 \\
\omega\mu_t Y_{z+} & \omega\mu_t Y_{z-} & -1 & 0 \\
-\frac{k_z^+}{\cos\theta_i} & -\frac{k_z^-}{\cos\theta_i} & 0 & -1 \\
\eta_0\omega\varepsilon_t & \eta_0\omega\varepsilon_t & 0 & -1 \\
-\frac{\eta_0 k_z^+ Y_{z+}}{\cos\theta_i} & -\frac{\eta_0 k_z^- Y_{z-}}{\cos\theta_i} & -1 & 0
\end{pmatrix} \tag{15}
$$

Thus, the reflection and transmission matrix of the uniaxial chiral slab can be obtained numerically from above Equations (14)–(15):

$$
\begin{pmatrix} E_{r\perp} \\ E_{r\parallel} \end{pmatrix} = \begin{bmatrix} R_{11} & R_{12} \\ R_{21} & R_{22} \end{bmatrix} \begin{pmatrix} E_{i\perp} \\ E_{i\parallel} \end{pmatrix} \tag{16}
$$

$$
\begin{pmatrix} E_{t\perp} \\ E_{t\parallel} \end{pmatrix} = \begin{bmatrix} T_{11} & T_{12} \\ T_{21} & T_{22} \end{bmatrix} \begin{pmatrix} E_{i\perp} \\ E_{i\parallel} \end{pmatrix} \tag{17}
$$

The normalized reflected power and transmitted power can be calculated from following formulas:

$P_r = |R_{11}|^2 + |R_{21}|^2$, $P_t = |T_{11}|^2 + |T_{21}|^2$, for TE incident wave, and

$P_r = |R_{12}|^2 + |R_{22}|^2$, $P_t = |T_{12}|^2 + |T_{22}|^2$, for TM incident wave, where $|R_{11}|^2$, $|T_{11}|^2$, $|R_{22}|^2$, and $|T_{22}|^2$ correspond to the co-polarized wave terms and $|R_{21}|^2$, $|T_{21}|^2$, $|R_{12}|^2$, and $|T_{12}|^2$ correspond to the cross-polarized wave terms.

3. NUMERICAL EXAMPLES AND DISCUSSION

In this section, we will present numerical examples for four cases of electromagnetic parameters of the uniaxial chiral slab: $\varepsilon_t > 0$, $\varepsilon_z > 0$; $\varepsilon_t < 0$, $\varepsilon_z > 0$; $\varepsilon_t > 0$, $\varepsilon_z < 0$; and $\varepsilon_t < 0$, $\varepsilon_z < 0$, and discuss the existence of the Brewster's angle for different chiral parameters. Here we assume $\mu_t = \mu_z = \mu_0$, $\omega/2\pi = 10\,\text{GHz}$, $d = 5\,\text{mm}$.

3.1. Case (A): $\varepsilon_t > 0$, $\varepsilon_z > 0$

Figures 2(a) and (b) show the normalized reflected and transmitted power versus incident angle θ_i for different chiral parameters $\kappa = 1e{-}6$, 0.5, 1.5, 3, where $\varepsilon_t = 3\varepsilon_0$, $\varepsilon_z = 4\varepsilon_0$. Solid and dashed lines correspond to TM (electric field parallel to the plane of incidence) and TE (electric field perpendicular to the plane of incidence) incident waves. It is found from the calculation that, for TM incident wave, the Brewster's angle $\theta_{B\|}$ (normalized reflected power equal to zero) exists only for smaller chiral parameters ($\kappa = 1e-6$ and $\kappa = 0.5$, black and red solid curves in Fig. 2(a)). With the increases of the chiral parameter, $\theta_{B\|}$ becomes bigger and then disappears ($\kappa = 1.5$, blue solid curve in Fig. 2(a)). When the chiral parameter becomes very large, the Brewster's angle $\theta_{B\|}$ occurs again ($\kappa = 3$, green solid curve in Fig. 2(a)). Its value is smaller than that for smaller chiral parameters. It is found from the calculation that the total of the normalized reflected and transmitted power is one, and it can also be seen from Figs. 2(a) and (b). At the

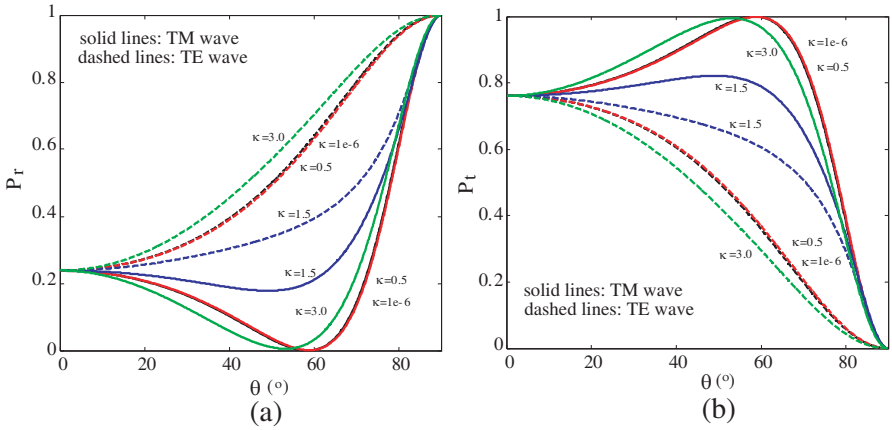

Figure 2. The normalized reflected power (a) and transmitted power (b) for TE (dashed lines), TM (solid lines) incident waves and different chiral parameters $\kappa = 1e-6$, 0.5, 1.5, 3, where $\varepsilon_t = 3\varepsilon_0$, $\varepsilon_z = 4\varepsilon_0$.

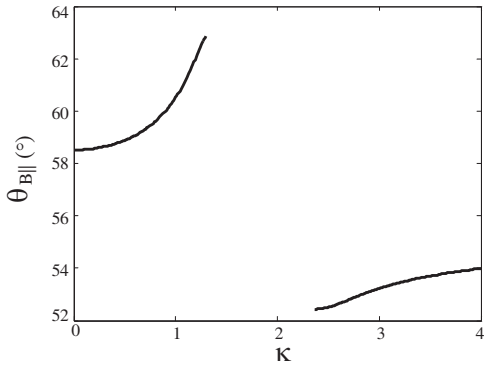

Figure 3. The Brewster's angle $\theta_{B\|}$ versus the chirality parameter, where $\varepsilon_t = 3\varepsilon_0$, $\varepsilon_z = 4\varepsilon_0$.

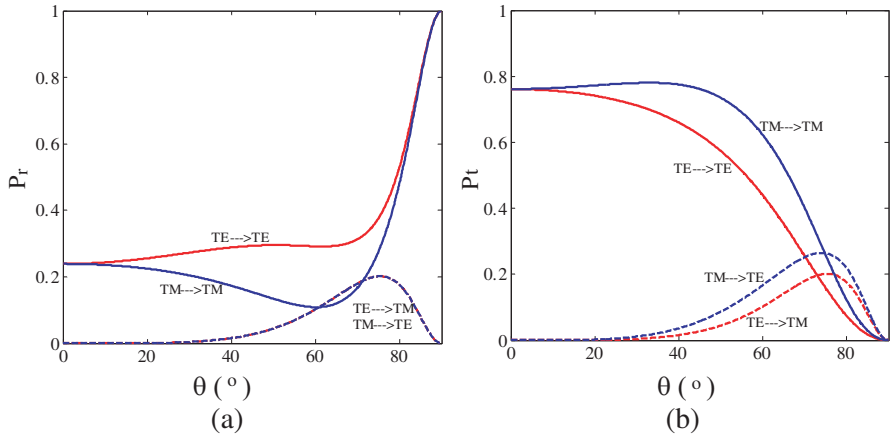

Figure 4. The power of the normalized reflected and transmitted co-polarized and cross-polarized waves for TE and TM incident waves, where $\varepsilon_t = 3\varepsilon_0$, $\varepsilon_z = 4\varepsilon_0$, $\kappa = 1.5$.

Brewster's angle $\theta_{B\|}$, the normalized transmitted power is equal to one, and total transmission will occur ($\kappa = 1e-6, 0.5, 3$ in Fig. 2(b)).

Figure 3 shows the Brewster's angle $\theta_{B\|}$ as a function of the chirality parameter, where $\varepsilon_t = 3\varepsilon_0$, $\varepsilon_z = 4\varepsilon_0$. When $\kappa < 1.3$ and $\kappa > 2.4$, the Brewster's angle $\theta_{B\|}$ exists, and increases with the chirality parameter increases. When $1.3 < \kappa < 2.4$, there is no Brewster's angle. In fact, when $1.3 < \kappa < 2.4$, only minimum reflection occurs, but no zero reflection.

For TE incident wave, the normalized reflected power increases with the incident angle θ_i increases for all chiral parameters. There is

no Brewster's angle appears for TE incident wave (Fig. 2(a)).

If we analyze the reflected and transmitted waves in detail, we can find that in the case of existence of the Brewster's angle, there is no cross-polarized wave appears in the reflected and transmitted wave when the incident wave is TE wave or TM wave. However, in the case of non-existence of the Brewster's angle, the cross-polarized waves will occur in the reflected and transmitted wave. That means if incident wave is TE wave, there are not only TE electromagnetic wave components but also TM components in the reflected and transmitted waves. For example, Figs. 4(a) and (b) illustrate the normalized reflected and transmitted co-polarized and cross-polarized waves power for TE and TM incident waves when the chiral parameter is $\kappa = 1.5$. The red solid and blue solid curves represent the power of co-polarized wave (TE to TE wave, TM to TM wave). The red dashed and blue dashed curves represent the power of cross-polarized waves (TE to TM wave, TM to TE wave). It can be seen from Fig. 4(a) that the power of the reflected cross-polarized waves are equal to each other (blue dashed curve in Fig. 4(a)). However, the power of the transmitted cross-polarized waves are different to each other (blue and red dashed curves in Fig. 4(b)).

3.2. Case (B): $\varepsilon_t < 0,\ \varepsilon_z > 0$

Figure 5 shows the normalized reflected power versus incident angle θ_i for different chiral parameters $\kappa = 1e-6, 0.5, 1.0$, where $\varepsilon_t = -4\varepsilon_0$, $\varepsilon_z = 0.5\varepsilon_0$. For TM incident wave, there exists the Brewster's angle for

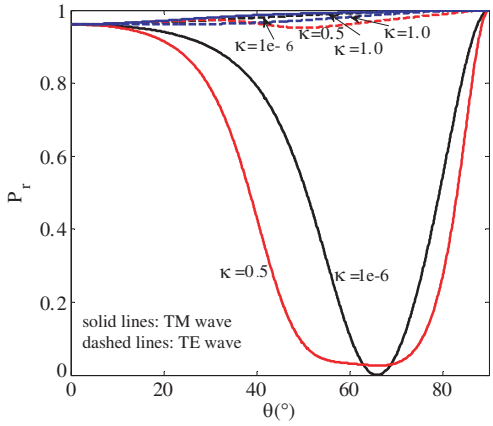

Figure 5. The normalized reflected power for different chiral parameters $\kappa = 1e-6$, 0.5, 1.0, where $\varepsilon_t = -4\varepsilon_0$, $\varepsilon_z = 0.5\varepsilon_0$.

smaller chiral parameter. With the increase of the chiral parameter, the Brewster's angle $\theta_{B\|}$ disappears ($\kappa = 0.5$, red solid curves in Fig. 5). The normalized reflected power is close to one for larger chiral parameter when incident angle θ_i is larger. Fig. 6 shows the Brewster's angle $\theta_{B\|}$ as a function of the chirality parameter, where $\varepsilon_t = -4\varepsilon_0$, $\varepsilon_z = 0.5\varepsilon_0$. When $\kappa < 0.45$, the Brewster's angle $\theta_{B\|}$ decreases with the chirality parameter increases. When $\kappa > 0.45$, the Brewster's angle disappears. For TE incident wave, almost total reflection occurs for arbitrary chiral parameter when incident angle θ_i is larger (dashed curves in Fig. 5).

3.3. Case (C): $\varepsilon_t > 0$, $\varepsilon_z < 0$

Figure 7 shows the normalized reflected power versus incident angle θ_i for different chiral parameters $\kappa = 1e-6$, 0.5, 1.5, 3.0, where $\varepsilon_t = 4\varepsilon_0$, $\varepsilon_z = -0.5\varepsilon_0$. There always exists Brewster's angle for TM incident wave. The Brewster's angle $\theta_{B\|}$ increases with chiral parameter κ increases. It is very interesting that the reflected power is nearly zero in some wide range of incident angle θ_i for smaller chiral parameters ($\kappa = 1e-6$ and 0.5, black and red solid curves in Fig. 7). That implies nearly total transmission can be achieved for wide range of incident angle θ_i. Fig. 8 shows the Brewster's angle $\theta_{B\|}$ as a function of the chirality parameter where $\varepsilon_t = 4\varepsilon_0$, $\varepsilon_z = -0.5\varepsilon_0$. The Brewster's angle $\theta_{B\|}$ increases with the chirality parameter increases. When the chirality parameter becomes very large, the Brewster's angle $\theta_{B\|}$ approaches 60 degree. For TE incident wave, the reflected power are almost the same for different chiral parameters.

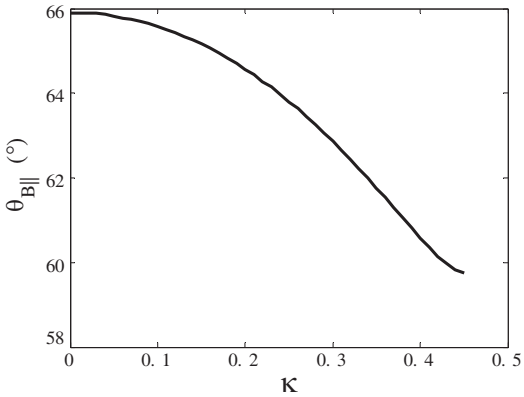

Figure 6. The Brewster's angle $\theta_{B\|}$ versus the chirality parameter, where $\varepsilon_t = -4\varepsilon_0$, $\varepsilon_z = 0.5\varepsilon_0$.

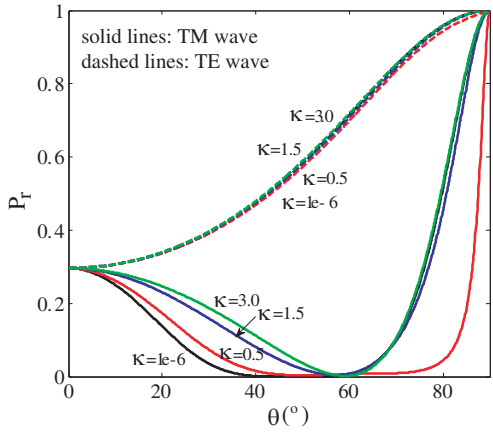

Figure 7. The normalized reflected power for different chiral parameters $\kappa = 1e-6,\ 0.5,\ 1.5,\ 3.0$, where $\varepsilon_t = 4\varepsilon_0$, $\varepsilon_z = -0.5\varepsilon_0$.

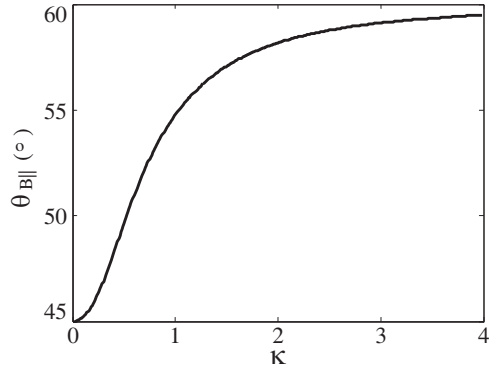

Figure 8. The Brewster's angle $\theta_{B\|}$ versus the chirality parameter where $\varepsilon_t = 4\varepsilon_0$, $\varepsilon_z = -0.5\varepsilon_0$.

3.4. Case (D): $\varepsilon_t < 0,\ \varepsilon_z < 0$

Figure 9 shows the normalized reflected power versus incident angle θ_i for different chiral parameters $\kappa = 1e{-}6,\ 0.5,\ 1.5,\ 3.0$, where $\varepsilon_t = -3\varepsilon_0$, $\varepsilon_z = -4\varepsilon_0$. There is no Brewster's angle and no total transmission regardless of the values of the chiral parameter for TE and TM incident wave. However, there are minimum values of the normalized reflected power for TM incident wave, and there are no minimum values for TE incident wave. The variation of the reflected power is small for different chiral parameters. The value of the normalized reflected power are large ($P_{\mathrm{r}} > 0.9$). It can be shown that refracted waves in

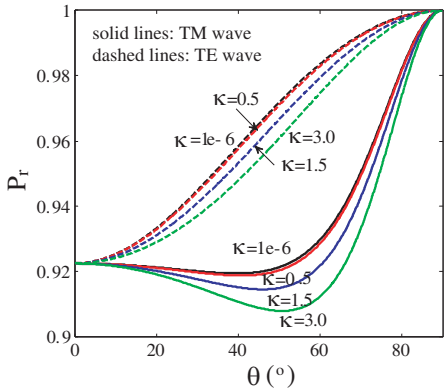

Figure 9. The normalized reflected power for different chiral parameters $\kappa = 1e-6$, 0.5, 1.5, 3.0, where $\varepsilon_t = -3\varepsilon_0$, $\varepsilon_z = -4\varepsilon_0$.

the uniaxial chiral slab become evanescent waves in the case of $\varepsilon_t < 0$ and $\varepsilon_z < 0$. There always exists little transmitted power, and most power is reflected, thus there is no Brewster's angle.

4. CONCLUSION

The reflection and transmission of electromagnetic waves by a uniaxially chiral slab with the optical axis perpendicular to the interface have been investigated. The formulas of the reflection and transmission are derived, numerical examples for four cases of electromagnetic parameters of uniaxial chiral slab are given, and different chiral parameters are considered. The existence of the Brewster's angles and total transmission are discussed. For the cases of $\varepsilon_t > 0$, $\varepsilon_z > 0$; $\varepsilon_t < 0$, $\varepsilon_z > 0$; and $\varepsilon_t > 0$, $\varepsilon_z < 0$; the Brewster's angles exist for TM incident wave. For the case of $\varepsilon_t < 0$, $\varepsilon_z < 0$, there is no Brewster's angles. Through the results presented here we may find potential applications for the design of microwave and optical devices such as polarization transformer.

ACKNOWLEDGMENT

This work is supported by the National Natural Science Foundation of China (61078060), the Natural Science Foundation of Zhejiang Province, China (Y1091139), Ningbo Optoelectronic Materials and Devices Creative Team (2009B21007), and is partially sponsored by K. C. Wong Magna Fund in Ningbo University.

REFERENCES

1. Pendry, J. B., "A chiral route to negative refraction," *Science*, Vol. 306, 1353–1355, 2004.
2. Tretyakov, S., A. Sihvola, and L. Jylhä, "Backward-wave regime and negative refraction in chiral composites," *Photonics and Nanostructures*, Vol. 3, Nos. 2–3, 107–115, 2005.
3. Mackay, T. G., "Plane waves with negative phase velocity in isotropic chiral mediums," *Microwave Opt. Tech. Lett.*, Vol. 45, No. 2, 120–121, 2005.
4. Plum, E., J. Zhou, J. Dong, V. A. Fedotov, T. Koschny, C. M. Soukoulis, and N. I. Zheludev, "Metamaterial with negative index due to chirality," *Phys. Rev. B*, Vol. 79, 035407, 2009.
5. Zhang, S., Y. Park, J. Li, X. Lu, W. Zhang, and X. Zhang, "Negative refractive index in chiral metamaterials," *Phys. Rev. Lett.*, Vol. 102, 023901, 2009.
6. Zhou, J., J. Dong, B. Wang, T. Koschny, M. Kafesaki, and C. M. Soukoulis, "Negative refractive index due to chirality," *Phys. Rev. B*, Vol. 79, 121104(R), 2009.
7. Wiltshire, M. C. K., J. B. Pendry, and J. V. Hajnal, "Chiral swiss rolls show a negative refractive index," *J. Phys.: Condens. Matter*, Vol. 21, No. 29, 292201, 2009.
8. Dong, J., J. Zhou, T. Koschny, and C. M. Soukoulis, "Bi-layer cross chiral structure with strong optical activity and negative refractive index," *Optics Express*, Vol. 17, No. 16, 14172–14179, 2009.
9. Li, J., F.-Q. Yang, and J. Dong, "Design and simulation of L-shaped chiral negative refractive index structure," *Progress In Electromagnetics Research*, Vol. 116, 395–408, 2011.
10. Wu, Z., B. Q. Zeng, and S. Zhong, "A double-layer chiral metamaterial with negative index," *Journal of Electromagnetic Waves and Applications*, Vol. 24, No. 7, 983–992, 2010.
11. Zarifi, D., M. Soleimani, and V. Nayyeri, "A novel dual-band chiral metamaterial structure with giant optical activity and negative refractive index," *Journal of Electromagnetic Waves and Applications*, Vol. 26, Nos. 2–3, 251–263, 2012.
12. Monzon, C. and D. W. Forester, "Negative refraction and focusing of circularly polarized waves in optically active media," *Phys. Rev. Lett.*, Vol. 95, 123904, 2005.
13. Jin, Y. and S. He, "Focusing by a slab of chiral medium," *Optics Express*, Vol. 13, No. 13, 4974–4979, 2005.

14. Qiu, C.-W., N. Burokur, S. Zouhdi, and L.-W. Li, "Chiral nihility effects on energy flow in chiral materials," *J. Opt. Soc. Am. A*, Vol. 25, No. 1, 55–63, 2008.
15. Dong, W., L. Gao, and C. W. Qiu, "Goos-Hänchen shift at the surface of chiral negative refractive media," *Progress In Electromagnetics Research*, Vol. 90, 255–268, 2009.
16. Cheng, X. X., H. S. Chen, B.-I. Wu, and J. A. Kong, "Visualization of negative refraction in chiral nihility media." *IEEE Antennas & Propagation Magazine*, Vol. 51, No. 4, 79–87, 2009.
17. Tuz, V. R. and C.-W. Qiu, "Semi-infinite chiral nihility photonics: Parametric dependence, wave tunneling and rejection," *Progress In Electromagnetics Research*, Vol. 103, 139–152, 2010.
18. Ahmed, S. and Q. A. Naqvi, "Electromagnetic scattering from a chiral-coated nihility cylinder," *Progress In Electromagnetics Research Letters*, Vol. 18, 41–50, 2010.
19. Naqvi, A., S. Ahmed, and Q. A. Naqvi, "Perfect electromagnetic conductor and fractional dual interface placed in a chiral nihility medium," *Journal of Electromagnetic Waves and Applications*, Vol. 24, Nos. 14–15, 1991–1999, 2010.
20. Huang, Y. Y., W. T. Dong, L. Gao, and D. W. Qiu, "Large positive and negative lateral shifts near pseudo-brewster dip on reflection from a chiral metamaterial slab," *Optics Express*, Vol. 19, No. 2, 1310–1323, 2011.
21. Qamar, S. R., A. Naqvi, A. A. Syed, and Q. A. Naqvi, "Radiation characteristics of elementary sources located in unbounded chiral nihility metamaterial," *Journal of Electromagnetic Waves and Applications*, Vol. 25, Nos. 5–6, 713–722, 2011.
22. Ahmad, F., S. N. Ali, A. A. Syed, and Q. A. Naqvi, "Chiral and/or chiral nihility interfaces: Parametric dependence, power tunneling and rejection," *Progress In Electromagnetics Research M*, Vol. 23, 167–180, 2012.
23. Jin, Y., J. He, and S. He, "Surface polaritons and slow propagation related to chiral media supporting backward waves," *Phys. Lett. A*, Vol. 351, Nos. 4–5, 354–358, 2006.
24. Dong, J. F., "Surface wave modes in chiral negative refraction grounded slab waveguides," *Progress In Electromagnetics Research*, Vol. 95, 153–166, 2009.
25. Dong, J. and C. Xu, "Characteristics of guided modes in planar chiral nihility metamaterial waveguides," *Progress In Electromagnetics Research B*, Vol. 14, 107–126, 2009.

26. Dong, J., "Exotic characteristics of power propagation in the chiral nihility fiber," *Progress In Electromagnetics Research*, Vol. 99, 163–178, 2009.
27. Dong, J., J. Li, and F.-Q. Yang, "Guided modes in the four-layer slab waveguide containing chiral nihility core," *Progress In Electromagnetics Research*, Vol. 112, 241–255, 2011.
28. Canto, J. R., C. R. Paiva, and A. M. Barbosa, "Dispersion and losses in surface waveguides containing double negative or chiral metamaterials," *Progress In Electromagnetics Research*, Vol. 116, 409–423, 2011.
29. Ye, Y. and S. He, "90° polarization rotator using a bilayered chiral metamaterial with giant optical activity," *Appl. Phys. Lett.*, Vol. 96, No. 20, 203501, 2010.
30. Sabah, C. and H. G. Roskos, "Design of a terahertz polarization rotator based on a periodic sequence of chiral-metamaterial and dielectric slabs," *Progress In Electromagnetics Research*, Vol. 124, 301–314, 2012.
31. Cheng, X. X., H. S. Chen, X. M. Zhang, B. L. Zhang, and B.-I. Wu, "Cloaking a perfectly conducting sphere with rotationally uniaxial nihility media in monostatic radar system," *Progress In Electromagnetics Research*, Vol. 100, 285–298, 2010.
32. Zarifi, D., H. Oraizi, and M. Soleimani, "Improved performance of circularly polarized antenna using semi-planar chiral metamaterial covers," *Progress In Electromagnetics Research*, Vol. 123, 337–354, 2012.
33. Lindell, I. V., A. H. Sihvola, S. A. Tretyakov, and A. J. Viitanen, *Electromagnetic Waves in Chiral and Bi-Isotropic Media*, Ch. 8, Artech House, Boston, London, 1994.
34. Bayatpur, F., A. V. Amirkhizi, and S. Nemat-Nasser, "Experimental characterization of chiral uniaxial bianisotropic composites at microwave frequencies," *IEEE Trans. Microwave Theory Tech.*, Vol. 60, No. 4, 1126–1135, 2012.
35. Cheng, Q. and T. J. Cui, "Negative refractions in uniaxially anisotropic chiral media," *Phys. Rev. B*, Vol. 73, 113104, 2006.
36. Cheng, Q. and T. J. Cui, "Reflection and refraction properties of plane waves on the interface of uniaxially anisotropic chiral media," *J. Opt. Soc. Am. A*, Vol. 23, No. 12, 3203–3207, 2006.
37. Dong, J. F. and J. Li, "Characteristics of guided modes in uniaxial chiral circular waveguides," *Progress In Electromagnetics Research*, Vol. 124, 331–345, 2012.

38. Silverman, M. P., "Reflection and refraction at the surface of a chiral medium: Comparison of gyrotropic constitutive relations invariant or noninvariant under a duality transformation," *J. Opt. Soc. Am. A*, Vol. 3, No. 6, 830–837, 1986.
39. Bassiri, S., C. H. Papas, and N. Engheta, "Electromagnetic wave propagation through a dielectric-chiral interface and through a chiral slab," *J. Opt. Soc. Am. A*, Vol. 5, No. 9, 1450–1459, 1988.
40. Bassiri, S., C. H. Papas, and N. Engheta, "Electromagnetic wave propagation through a dielectric-chiral interface and through a chiral slab: Errata," *J. Opt. Soc. Am. A*, Vol. 7, No. 11, 2154–2155, 1990.
41. Cory, H. and I. Rosenhouse, "The reflection and transmission of electromagnetic waves by a chiral slab," *J. Mod. Opt.*, Vol. 39, No. 6, 1321–1330, 1992.
42. Bahar, E., "Mueller matrices for waves reflected and transmitted through chiral materials: Waveguide modal solutions and applications," *J. Opt. Soc. Am. B*, Vol. 24, No. 7, 1610–1619, 2007.
43. Menzel, C., C. Rockstuhl, T. Paul, and F. Lederer, "Retrieving effective parameters for quasiplanar chiral metamaterials," *Appl. Phys. Lett.*, Vol. 93, No. 23, 233106, 2008.
44. Semchenko, I. V., S. A. Khakhomov, S. A. Tretyakov, A. H. Sihvola, and E. A. Fedosenko, "Reflection and transmission by a uniaxially bi-anisotropic slab under normal incidence of plane waves," *J. Phys. D: Appl. Phys.*, Vol. 31, No. 19, 2458–2464, 1998.
45. Uckun, S., "Plane wave propagation through a uniaxial chiral slab and transmission coefficient," *Microwave Opt. Tech. Lett.*, Vol. 18, No. 3, 171–174, 1998.
46. Viitanen, A. J. and I. V. Lindell, "Uniaxial chiral quarter-wave polarisation transformer," *Electron. Lett.*, Vol. 29, No. 12, 1074–1075, 1993.